Progress In Electromagnetics Research M, Vol. 31, 59–69, 2013

DUAL-BAND TERAHERTZ CHIRAL METAMATERIAL WITH GIANT OPTICAL ACTIVITY AND NEGATIVE REFRACTIVE INDEX BASED ON CROSS-WIRE STRUCURE

Fang Fang[1] and Yongzhi Cheng[2, *]

[1]College of Information Engineering, Hubei Institute for Nationalities, Enshi 44500, China

[2]School of Optical and Electronic Information, Huazhong University of Science and Technology, Wuhan 430074, China

Abstract—In this paper, a dualband chiral metamaterial (CMM) based on cross-wire structure is proposed and studied numerically. It exhibits dual-band giant optical activity and negative refractive index in terahertz region. The surface current distributions are calculated to explain original physics. The further numerical results show that the effective frequency bands of the CMMs can be independent adjusted easily by changing the structure geometrical parameter. The designed dual-band terahertz CMMs offer flexibility in the investigation of novel terahertz device application.

1. INTRODUCTION

Electromagnetic (EM) metamaterials (MMs) are manmade effective media composed of sub-wavelength metallic structure or dielectric elements and exhibit exotic EM properties which cannot be encountered in nature [1]. Recently, more and more interest has been focused on the CMMs structures due to their attractive physical properties such as giant optical activity, strong circular dichroism (CD) effect, and negative refractive index (NRI) [2–10]. CMMs are MMs composed of unit cells without any mirror symmetry, where a magnetic or electric moment can be excited by the parallel external electric or magnetic field of the incident EM waves at the resonance. Thus, the degeneracy of the two circularly polarized waves is broken, i.e.,

Received 24 April 2013, Accepted 22 May 2013, Scheduled 29 May 2013

* Corresponding author: Yongzhi Cheng (cyz0715@126.com).

refractive indices of right circularly polarized (RCP, +) waves and left circularly polarized (LCP, −) waves are different.

According to the chiral media constitutive relations, the refractive indices for RCP and LCP waves are expressed as $n_{\pm} = n \pm \kappa$, which implies that the negative of n_+ or n_- is possible provided a large enough chirality in principle [3]. Where $n = \sqrt{\varepsilon\mu}$, ε and μ are the relative permittivity and permeability of the CMMs, κ is the chiral parameter. For general bi-layer CMMs, the CD effect and optical activity are important EM properties [7]. The CD denotes different absorptivity of a RCP and LCP wave inside the CMMs, which can be expressed as $\Delta = |T_{++}| - |T_{--}|$, where T_{++} and T_{--} are the RCP and LCP transmission coefficients. While the ellipticity defines the difference of polarization state of transmitted waves and incident waves, which can be expressed as $\eta = \arctan[(|T_{++}| - |T_{--}|)/(|T_{++}| + |T_{--}|)]$. The optical activity mainly characterizes the rotation angle between the polarization planes of the transmitted and incident waves and can be expressed as $\theta = [\arg(T_{++}) - \arg(T_{--})]/2$. Various enantiomeric forms bi-layer planar chiral structure have been proposed and investigated widely, such as twist rosettes [7], twist cross wires [3, 11, 13], U shape SRRs [14], conjugate swastikas [15, 16], and other novel bi-layer structures [17–24], which could exhibit negative refractive index and optical activity in a single frequency band or dual-band. More recently, negative refractive index of 3 dimensional compact helix structures also has been investigated in microwave frequency [25–27], however, which is hard to fabricate and integrate into present systems, especially in teraherz (THz) and optical region. THz is a unique frequency range which has attracted significant attention due to its potential applications in sensing, biomedical imaging, and wireless communication, among others [5, 28]. Because of the lack of natural materials for manipulating the THz wave, the development of MMs with unusual optical properties for this frequency region is especially important [29, 30].

In this work, we propose a dual-band THz CMMs with combined two different sized cross-wire structures in a unit cell. The stronger CD effect, giant optical activity and multiple negative refractive index bands could be obtained by numerical simulations based on the frequency domain finite element method. The resonances mechanism could be further illustrated by simulated surface current distributions. The further simulated results show that the effective frequency bands of this structure and can be simply adjusted. These results can give a more profound understanding on chirality and to offer flexibility in the investigation of novel terahertz device.

2. STRUCTURE DESIGN AND SIMULATION

The dependences of optical properties of the bi-layer twisted cross-wire structure to the structural parameters in infrared region have been studied systematically [11]. It can be found that the functional frequency region of the CMMs could be adjusted easily by changing the dielectric layer thickness and width of cross-wire. The exceptional strong polarization rotation, CD effect and negative refractive index also could be found by selecting these structure parameters appropriately. Based on this idea, to obtain dual-bands resonances, we can combine two different sized cross-wire structures in a unit cell.

The unit cell of dual-band THz CMMs is composed of two different sized mutually twisted metallic cross-wire separated by dielectric layer. The schematic of the unit cell is depicted in Fig. 1. We selected 0.2 μm thick gold film as metallic material since it has the smallest loss in terahertz and higher frequency region. Computer numerical simulations were performed based on the frequency domain finite element method by CST Microwave Studio software. In simulations, the unit cell boundary condition was applied and the circular polarized eigenwaves were used directly. In simulation model, we also use benzocyclobutene (BCB) with the relative dielectric constant of 2.67 as the isotropic dielectric spacer, and the gold is described by the frequency dependent Drude model with plasma frequency $w_p = 1.37 \times 10^{16}\,\mathrm{s}^{-1}$ and scattering frequency $\gamma = 2.04 \times 10^{14}\,\mathrm{s}^{-1}$ [5, 31].

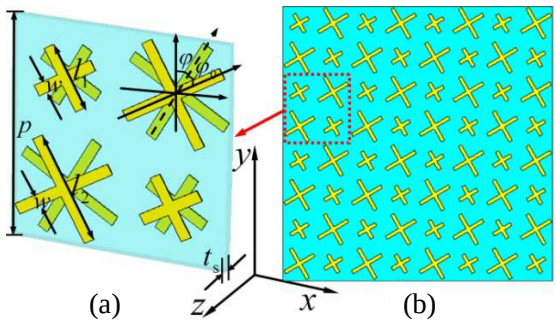

Figure 1. The schematic of designed bi-layer CMMs. (a) Perspective view of unit cell. (b) Two-dimensional array. The geometrical parameters of this CMMs are $t_s = 1.6\,\mu\mathrm{m}$, $p = 40\,\mu\mathrm{m}$, $w = 2\,\mu\mathrm{m}$, $l_1 = 12\,\mu\mathrm{m}$, $l_2 = 18\,\mu\mathrm{m}$, $\varphi = \varphi_0 = 30^\circ$.

3. RESULTS AND DISCUSSION

The simulation results of RCP and LCP transmission coefficients are illustrated in Fig. 2(a). There exist four obvious transmission resonant frequencies: $f_1 = 4.8\,\text{THz}$, $f_2 = 5.6\,\text{THz}$, $f_3 = 7.9\,\text{THz}$ and $f_4 = 8.2\,\text{THz}$ for LCP and RCP waves, respectively. It should be noticed that four resonances occurred with giant CD effect, i.e., the resonance of one circular polarization is more pronounced than that of the other one. We can conjecture that the two resonances are corresponding to smaller size cross-wire structure, and the other two resonances are to the bigger one. As shown in Fig. 2(b), in the first and fourth resonant frequencies, i.e., 4.8 THz, and 8.2 THz, the transmission of RCP wave is about 13.5 dB and 5.7 dB higher than that of LCP wave, respectively. While in the second and third resonant frequency of 5.6 THz and 7.9 THz, the transmission of RCP wave is about 8.7 dB and 15.3 dB lower than that of LCP wave. Thus, we can obtain the maximal CD parameter 15.3 dB around 12.1 THz, which indicates the giant CD effect.

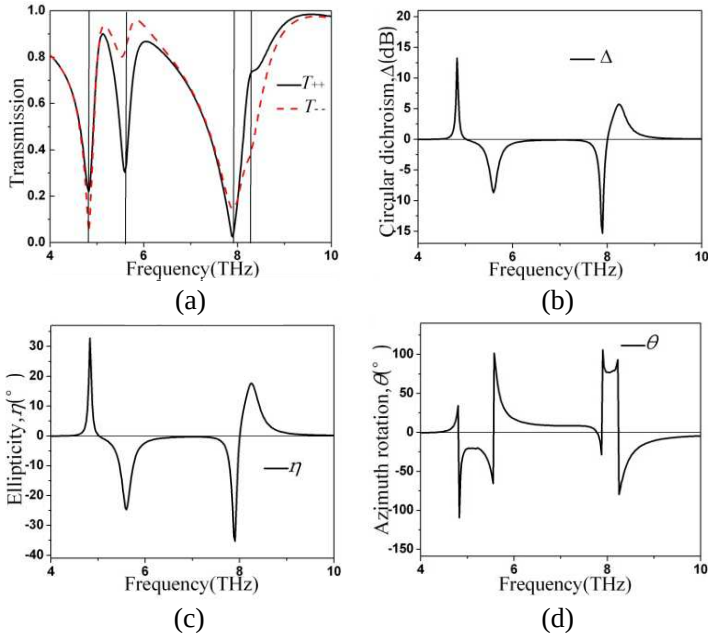

Figure 2. (a) Simulated transmission coefficients (T_{++}, T_{--}). (b) The circular dichroism (Δ). (c) The ellipticity angle (η). (d) Polarization azimuth rotation angle (θ).

The ellipticity angle (η) and polarization azimuth rotation angle (θ) of the transmitted wave were calculated according to above equations, respectively, and results are shown in Figs. 2(c) and (d). It can be seen that the η is up to maximal values $-24.9°$, $7.4°$, $-16.6°$ and $-29.9°$ at resonant frequencies of 4.8 THz, 5.6 THz, 7.9 THz and 8.2 THz, respectively. The θ is also up to maximal values $-109.3°$, $101.6°$, $105.9°$ and $93.2°$ at the same resonant frequencies, respectively. It can be noticed that far from the resonant frequencies, a significant difference between the phases of the RCP and LCP transmission is observed, which causes the pure rotation of the polarization plane of a linearly polarized wave propagating through the designed CMMs structure. At the frequencies of 5 THz and 8 THz, we obtain $\eta = 0$ where it corresponds to a pure optical activity, which means that the incident wave is linearly polarized, the transmitted wave is still linearly polarized but with a rotated angle θ. The azimuth rotation angle θ is approximately $-20.3°$ and $76.9°$ for 2 µm thick CMMs (i.e., the rotation angle is about $609°/\lambda$ and $1441.9°/\lambda$ at 5 THz and 8 THz, respectively). The proposed CMMs structure exhibits stronger optical activity compared with the previously reported CMMs designs in higher frequency band (around 8 THz) [3–5, 11–21].

Taking a further, after obtaining the data of the simulation transmissions and reflections, we calculated the effective EM parameters by using a standard parameter retrieval procedure [3, 7]. To illustrate the exotic EM properties clearly and simply, we only present the real part of the effective EM parameters of the proposed structure. As shown in Fig. 3(a), similar to the previous designed novel dual-band structure [20], the real part of chiral parameter Re(κ)

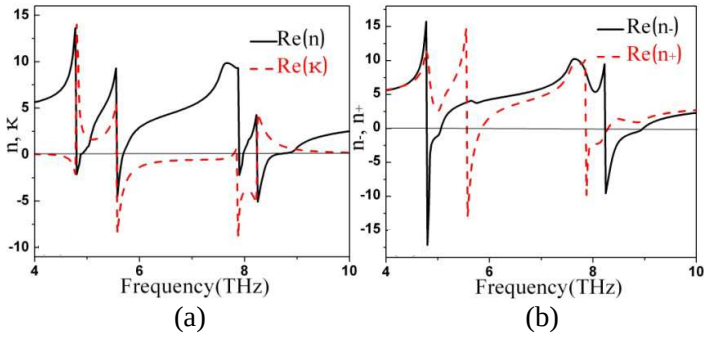

Figure 3. (a) The real parts of chiral parameter Re(κ) and refractive index Re(n). (b) The real parts of refractive index for LCP and RCP waves Re(n_+) and Re(n_-).

curve also exhibits four resonances; the first couple is 4.8 THz and 5.6 THz, and the second one is 7.9 THz and 8.2 THz. At these resonant frequencies, the Re(κ) is up to maximal values 13.6, -8.4, -8.9, and -5.2, respectively. At the same time, we can obtain four maximal negative Re(n) (about -2.1, -4.1, -2.2, and -5.1) at these resonant frequencies, which indicate that the proposed MMs can achieve dual-band negative refractive properties in THz region. The generations of the negative refractive indices are mainly due to the high chirality of the designed structure [3, 24]. Generally, we can use the effective loss factor characterize how well the MMs behaves. The effective loss factor can be expressed as LF = $|\mathrm{Im}(n)/\mathrm{Re}(n)|$ for average refractive index, and the loss factor of RCP and LCP can be expressed as LF = $|\mathrm{Im}(n_{\pm})/\mathrm{Re}(n_{\pm})|$ [23, 24]. The LF of the effective refractive index is less than 0.2 at resonances, which indicated that the loss of the proposed dual-band CMMs is relative small. As shown in Fig. 3(b), due to the relation of $n_{\pm} = n \pm \kappa$, the strong chirality could push the refractive index from positive to negative values for the RCP and LCP waves around resonant frequencies, respectively. It is seen that above the first and fourth resonant frequencies, n_{-} is negative from 4.8 to 5.1 THz, and 8.2 to 9 THz, respectively. Similarly, above the second and third resonant frequencies, n_{+} is negative from 5.6 to 5.9 THz, and 7.8 to 8.2 THz respectively. Thus, it is obvious that the effective negative reflective index originates from chiral configuration of this MMs.

The real parts of the retrieved effective permittivity Re(ε) and permeability Re(μ) as a function of frequency for the proposed CMMs structure are presented in Fig. 4. There are obvious resonances on the Re(ε) and (Reμ) curves, which are corresponding to the four resonant

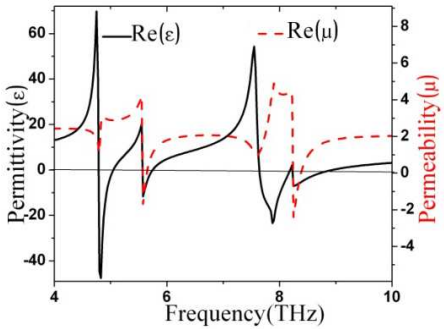

Figure 4. The real parts of effective permittivity Re(ε) and effective permeability Re(μ).

frequencies of the κ curve. It is seen that $\mathrm{Re}(\varepsilon)$ is negative around the four resonant frequencies, while the $\mathrm{Re}(\mu)$ is negative only at second and fourth resonant frequencies. This will not result in a negative refractive index in traditional MMs. Thus, the negative refractive indices of RCP and LCP waves are actually attributed to the relatively small refractive index and large chirality.

The mechanism of the resonances for the proposed dual-band CMMs can be better understood by studying the surface current distributions on the upper and bottom patterns of the proposed CMMs structure for the RCP and LCP waves at resonances. As shown in Fig. 5, obviously, the first couple resonances (4.8 THz and 5.6 THz) are mainly caused by the longer bi-layer cross-wire structure, while the second couple resonances (7.9 THz and 8.2 THz) are mainly attributed to the shorter one. From Figs. 5(a) and 4(c), at the resonances (4.8 THz and 7.9 THz), one can see parallel currents flowing on the two layers for both longer and short cross-wires, which are symmetric current resonance modes and indicated stronger electrical resonances. While at 5.6 THz and 8.2 THz, we can see that the antiparallel exist on the top and bottom layer for longer and short cross-wires pairs, which are asymmetric resonance modes and indicated stronger magnetic resonances. The surface current distributions features are similarly to the previous single cross-wire structure in gigahertz frequency range, the different sized cross-wire pairs also can be viewed as chiral version of the short wire pairs, which has similar current distributions in the symmetric and asymmetric resonance modes [3]. These magnetic and electric resonances are also consistent with the retrieval effective permeability and permittivity as shown in Fig. 4.

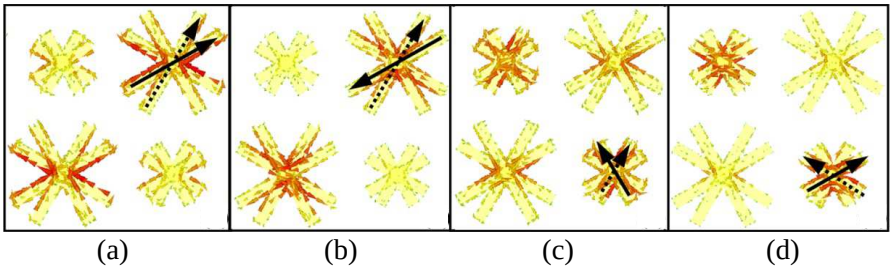

Figure 5. (a) The surface current distributions on the upper and bottom patterns of the proposed CMMs structure for the RCP waves at (a) 4.8 THz and (d) 8.2 THz, and for the LCP waves at (b) 5.6 THz and (c) 7.9 THz, respectively. The long solid (dashed) arrows represent the front (back) surface current directions.

Numerical results show that the effective frequency bands of the CMMs can be independent adjusted easily by changing the structure geometrical parameter. If we keep the length of one cross-wire structure unchanged and vary the length of the other one, the one frequency band will be fixed and the other one will change. To further illustrate this conjecture, the dependences of resonant frequencies with parameter l_1 shown in Fig. 1(a) are presented in Fig. 6. It can be clearly seen that, with variation of l_1 from 10 to 18 μm, the first couple resonant frequencies (i.e., the first and second resonant frequencies) are nearly unchanged, while the second couple resonant frequencies change from 8.45 to 6.05 THz and 8.83 to 6.65 THz, respectively. The presented simulated results indicate that this scheme could be used to design other dual-band or multi-band CMMs.

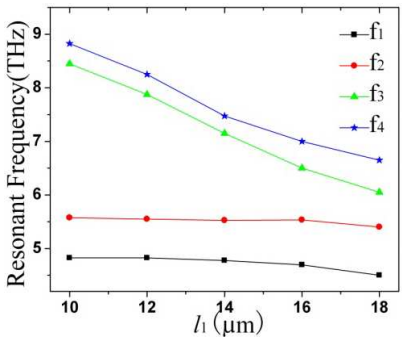

Figure 6. Dependences of resonant frequencies of the dual-band CMMs structure with length l_1 of short cross-wire.

4. CONCLUSION

In conclusion, a dual-band THz CMMs is proposed by combining two different size cross-wire structures in each unit cell. The results show that the dual-band giant optical activity and negative refractive indices are observed in THz region by numerical simulation and standard parameter retrieval procedure. We observe a polarization rotation angle of 76.9° with $\eta = 0$ for the proposed CMMs, which is larger than the current reported chiral structure. We can obtain four maximal values -2.1, -4.1, -2.2, and -5.1 of effective refractive indices at 4.8 THz, 5.6 THz, 7.9 THz and 8.2 THz, respectively. The surface current distributions are studied to understand the mechanism of the resonances. In addition, it is expected to design a multi-band CMM structure based on this idea. Therefore, the findings are important for

the development of CMMs which may have many potential applications in the THz frequency range, such as wave plate, ultrathin polarizer, band pass filters, and others.

REFERENCES

1. Veselago, V. G., "The electrodynamics of substances with simultaneously negative values of ε and μ," *Sov. Phys. Usp.*, Vol. 10, No. 4, 509–514, 1968.
2. Pendry, J. B., "A chiral route to negative refraction," *Science*, Vol. 306, 1353, 2004.
3. Zhou, J., J. Dong, B. Wang, T. Koschny, M. Kafesaki, and C. M. Soukoulis, "Negative refractive index due to chirality," *Phys. Rev. B*, Vol. 79, 121104, 2009.
4. Rogacheva, A. V., V. A. Fedotov, A. S. Schwanecke, and N. I. Zheludev, "Giant gyrotropy due to electromagnetic-field coupling in a bilayered chiral structure," *Phys. Rev. Lett.*, Vol. 97, 177401, 2006.
5. Zhang, S., Y. S. Park, J. Li, X. Lu, W. Zhang, and X. Zhang, "Negative refractive index in chiral metamaterials," *Phys. Rev. Lett.*, Vol. 102, 023901, 2009.
6. Feng, C., Z. B. Wang, S. Lee, J. Jiao, and L. Li, "Giant circular dichroism in extrinsic chiral metamaterials excited by off-normal incident laser beams," *Opt. Communications*, Vol. 285, 2750, 2012.
7. Wang, B., J. Zhou, T. Koschny, M. Kafesaki, and C. M. Soukoulis, "Chiral metamaterials: Simulations and experiments," *J. Opt. A: Pure Appl. Opt.*, Vol. 11, 114003, 2009.
8. Rogacheva, A. V., V. A. Fedotov, A. S. Schwanecke, and N. I. Zheludev, "Giant gyrotropy due to electromagnetic-field coupling in a bilayered chiral structure," *Phys. Rev. Lett.*, Vol. 97, No. 17, 177401, 2006.
9. Canto, J. R., C. R. Paiva, and A. M. Barbosa, "Dispersion and losses in surface waveguides containing double negative or chiral metamaterials," *Progress In Electromagnetics Research*, Vol. 116, 409–423, 2011.
10. Sabah, C. and H. G. Roskos, "Design of a terahertz polarization rotator based on a periodic sequence of chiral-metamaterial and dielectric slabs," *Progress In Electromagnetics Research*, Vol. 124, 301–314, 2012.
11. Plum, E., J. Zhou, J. Dong, V. A. Fedotov, T. Koschny, C. M. Soukoulis, and N. I. Zheludev, "Metamaterial with negative

index due to chirality," *Phys. Rev. B*, Vol. 79, No. 3, 035407(6), 2009.

12. Dong, J., J. Zhou, T. Koschny, and C. Soukoulis, "Bi-layer crosschiral structure with strong optical activity and negative refractiveindex," *Optics Express*, Vol. 17, No. 16, 14172–14179, 2009.
13. Li, Z., H. Caglayan, E. Colak, J. Zhou, C. M. Soukoulis, and E. Ozbay, "Coupling effect between two adjacent chiral structure layers," *Optics Express*, Vol. 18, 5375, 2010.
14. Li, Z., R. Zhao, T. Koschny, M. Kafesaki, K. B. Alici, E. Colak, H. Caglayan, E. Ozbay, and C. M. Soukoulis, "Chiral metamaterials with negative refractive index based on four "U" split ring resonators," *Appl. Phys. Lett.*, Vol. 97, 081901, 2010.
15. Zhao, R., L. Zhang, J. Zhou, T. Koschny, and C. M. Soukoulis, "Conjugated gammadion chiral metamaterial with uniaxial optical activity and negative refractive index," *Phys. Rev. B*, Vol. 83, No. 3, 035105(4), 2011.
16. Zhou J., D. R. Chowdhury, R. Zhao, A. K. Azad, H. Chen, C. M. Soukoulis, A. J. Taylor, and J. F. O'Hara, "Terahertz chiral metamaterials with giant and dynamically tunable optical activity," *Phys. Rev. B*, Vol. 86, 035448, 2012.
17. Wu, Z., B. Q. Zhang, and S. Zhong, "A double-layer chiral metamaterial with negative index," *Journal of Electromagnetic Waves and Applications*, Vol. 24, No. 7, 983–992, 2010.
18. Li, J., F. Q. Yang, and J. F. Dong, "Design and simulation of L-shaped chiral negative refractive index structure," *Progress In Electromagnetics Research*, Vol. 116, 395–408, 2011.
19. Li, Z., K. B. Alici, E. Colak, and E. Ozbay, "Complementary chiral metamaterials with giant optical activity and negative refractive index," *Appl. Phys. Lett.*, Vol. 98, 161907, 2011.
20. Zarifi, D., M. Soleimani, and V. Nayyeri, "A novel dual-band chiral metamaterial structure with giant optical activity and negative refractive index," *Journal of Electromagnetic Waves and Applications*, Vol. 26, Nos. 2–3, 251–263, 2012.
21. Cheng, Y. Z., Y. Nie, L. Wu, and R. Z. Gong, "Giant circular dichroism and negative refractive index of chiral metamaterial based on split-ring resonators," *Progress In Electromagnetics Research*, Vol. 138, 421–432, 2013.
22. Cheng, Y. Z., Y. Nie, and R. Z. Gong, "Giant optical activity and negative refractive index using complementary U-shaped structure assembly," *Progress In Electromagnetics Research M*, Vol. 25, 239–

253, 2012.

23. Matra, K. and N. Wongkasem, "Left-handed chiral isotropic metamaterials: Analysis and detailed numerical study," *J. Opt. A: Pure Appl. Opt.*, Vol. 11, 074011, 2009.
24. Panpradit, W., A. Sonsilphong, C. Soemphol, and N. Wongkasem, "High negative refractive index in chiral metamaterial," *J. Opt.*, Vol. 14, 075101, 2012.
25. Wongkasem, N., C. Kamtongdee, A. Akyurtlu, and K. A. Marx, "Artificial multiple helices: Polarization and EM properties," *J. Opt.*, Vol. 12, 075102, 2010.
26. Sonsilphong, A. and N. Wongkasem, "Three-dimensional artificial double helices with high negative refractive index," *J. Opt.*, Vol. 14, 105103, 2012.
27. Sonsilphong, A. and N. Wongkasem, "Low loss circular birefringence in artificial triple helices," *Progress In Electromagnetics Research M*, Vol. 29, 267–278, 2013.
28. Zhang, X. C., "Terahertz wave imaging: Horizons and hurdles," *Phys. Med. Biol.*, Vol. 47, 3667, 2002.
29. Andres-Garcia, B., L. E. Garcia-Munoz, V. Gonzalez-Posadas, F. J. Herraiz-Martinez, and D. Segovia-Vargas, "Filtering lens structure based on SRRs in the low THz band," *Progress In Electromagnetics Research*, Vol. 93, 71–90, 2009.
30. Guo, W., L. He, B. Li, T. Teng, and X. W. Sun, "A wideband and dual-resonant terahertz metamaterial using a modified SRR structure," *Progress In Electromagnetics Research*, Vol. 134, 289–299, 2013.
31. Ding, Y., G. Zhang, and Y. Cheng, "Giant optical activity and negative refractive index in the terahertz region using complementary chiral metamaterials," *Phys. Scr.*, Vol. 85, 065405, 2012.